




CISM COURSES AND LECTURES NO. 469
INTERNATIONAL CENTRE FOR MECHANICAL SCIENCES

PARAMETER IDENTIFICATION OF MATERIALS AND STRUCTURES

EDITED BY

ZENON MRÓZ
GEORGIOS E. STAVROULAKIS

 SpringerWienNewYork

CISM COURSES AND LECTURES

Series Editors:

The Rectors

Manuel Garcia Velarde - Madrid

Jean Salençon - Palaiseau

Wilhelm Schneider - Wien

The Secretary General

Bernhard Schrefler - Padua

Executive Editor

Carlo Tasso - Udine

The series presents lecture notes, monographs, edited works and proceedings in the field of Mechanics, Engineering, Computer Science and Applied Mathematics.

Purpose of the series is to make known in the international scientific and technical community results obtained in some of the activities organized by CISM, the International Centre for Mechanical Sciences.

INTERNATIONAL CENTRE FOR MECHANICAL SCIENCES

COURSES AND LECTURES - No. 469



PARAMETER IDENTIFICATION
OF MATERIALS AND STRUCTURES

EDITED BY

ZENON MRÓZ
TECHNICAL UNIVERSITY OF WARSAW, POLAND

GEORGIOS E. STAVROULAKIS
UNIVERSITY OF IOANNINA, GREECE
AND
TECHNICAL UNIVERSITY OF BRAUNSCHWEIG, GERMANY

SpringerWienNewYork

The publication of this volume was co-sponsored and co-financed by the UNESCO Venice Office - Regional Bureau for Science in Europe (ROSTE) and its content corresponds to a CISM Advanced Course supported by the same UNESCO Regional Bureau.

This volume contains 180 illustrations

This work is subject to copyright.
All rights are reserved,
whether the whole or part of the material is concerned
specifically those of translation, reprinting, re-use of illustrations,
broadcasting, reproduction by photocopying machine
or similar means, and storage in data banks.
© 2005 by CISM, Udine
Printed in Italy
SPIN 11583752

In order to make this volume available as economically and as rapidly as possible the authors' typescripts have been reproduced in their original forms. This method unfortunately has its typographical limitations but it is hoped that they in no way distract the reader.

ISBN-10 3-211-30151-8 SpringerWienNewYork
ISBN-13 978-3-211-30151-7 SpringerWienNewYork

PREFACE

The nature and the human creations are full of complex phenomena, which sometimes can be observed but rarely follow our hypotheses. The best we can do is to build a parametric model and then try to adjust the unknown parameters based on the available observations. This topic, called parameter identification, is discussed in this book for materials and structures.

The present volume of lecture notes follows a very successful advanced school, which we had the honor to coordinate in Udine, October 6-10, 2003. The authors of this volume present a wide spectrum of theories, methods and applications related to inverse and parameter identification problems.

We thank the invited lecturers and the authors of this book for their contributions, the participants of the course for their active participation and the interesting discussions as well as the people of CISM for their hospitality and their well-known professional help.

*Zenon Mróz
Georgios E. Stavroulakis*

CONTENTS

Preface

An overview of enhanced modal identification <i>by L. Bolognini</i>	1
The reciprocity gap functional for identifying defects and cracks <i>by H.D. Bui, A. Constantinescu and H. Maigre</i>	17
Some innovative industrial prospects centered on inverse analyses <i>by G. Maier, M. Bocciarelli and R. Fedele</i>	55
Identification of damage in beam and plate structures using parameter dependent modal changes and thermographic methods <i>by Z. Mróz and K. Dems</i>	95
Crack and flaw identification in statics and dynamics, using filter algorithms and soft computing <i>by G.E. Stavroulakis, M. Engelhardt and H. Antes</i>	139
Application of advanced optimization techniques to parameter and damage identification problems <i>by V. Toropov and F. Yoshida</i>	177
Neural networks in the identification analysis of structural mechanics problems <i>by Z. Waszczyszyn and L. Ziemianski</i>	265

An Overview of Enhanced Modal Identification

Luca Bolognini¹

¹ RSI Sistemi s.p.a., Altran Group, Milan, Italy

Abstract. The application of identification techniques is spreading in many engineering fields, as a reliable and realistic understanding of structures is becoming a common issue. The aim of this paper is to summarize the main steps needed for a complete and up-to-date identification process, referring to the modal approach. The complex eigenvalue approach and a non-proportional damping model are discussed in detail.

1 Why Identification

The construction industry is increasingly involved in the survey, assessment, alteration or refurbishment of existing structures. This is due to limited space and funds for new construction, the disruption costs, a greater environmental awareness and a cultural desire to maintain ancient and historic structures. At the same time, managing and operation of those structures having high social and economical impact (such as bridges, dams, commercial facilities) are demanding reliable condition-based safety evaluations.

Theoretical models of civil engineering structures are essential for assessment and for the design of alterations. For older structures these models often do not exist. Where they do exist (mostly based on visual survey) they are often inaccurate, and anyway “as-built” information often does not accurately reflect the work done on site.

Given the shortcomings in design data and surveys as a basis for structural models, it is clear that better non-destructive methods are needed for creating reliable models that accurately reflect the form and condition of existing structures. This process of adapting theoretical, approximate models to accord with observed behaviour is called structural identification.

It can be used for the most general structural component (in both mechanical and civil fields) with the main purpose of:

- improving the design stage (virtual modelling);
- enhancing the safety assessments;
- monitoring the evolution of structural conditions;
- evaluating the effect of modifications or refurbishment

The modal approach (aiming to the identification of structural intrinsic properties such as frequencies, modal deformations, damping factors and non linear behaviours) is one of the possible techniques that can be used for the purpose.

Many efforts have been spent to make this kind of identification general, reliable and easy to manage. In the following, a short excursus in the up-to-date modal identification practice will be given, with a few more detail as far as the complex approach and a non-proportional damping model are concerned.

2 The Identification Process

The identification basic idea is to improve our knowledge on a given structure through a model that accords with observed behaviour. In other words, to meet the real structure with its virtual modelling. The main steps of a complete identification process are summarized below.

- Starting from the Real Structure (Step 1),
- a Finite Element Model is defined (Step 2).
- To understand the structure's dynamic behaviour some Preliminary Modal Analyses are performed (Step 3) and
- the sensors lay-out is optimised by means of a Data Acquisition Planning (Step 4).
- It is then possible to get the experimental data, Testing the Structure (Step 5).
- Raw data are processed performing the Experimental Modal Analysis (Step 6), to derive the dynamic features of the real structures, which are compared with those obtained from the Finite Element model.
- The discrepancies are minimised modifying the material parameter values via the Modal Matching / Model Updating iterative procedure (Step 7).

The identification loop aims to a better understanding of the structure's current state and a more realistic model. In this view, many of the concepts hold for any other approach, substituting the modal one.

2.1 The Real Structure

The starting point of any identification process is the structure as such (Step 1). The safety assessment of a given structure starts from a correct interpretation of its actual status.



Figure 1. A typical example of structure to be identified: a masonry arch bridge. The geometrical shape can be correctly captured, different cortical construction materials can be mapped by visual inspection and boreholes can be used for fillings.

The behaviour of any structure is mainly a function of:

- the geometrical shape;
- the materials it is made of;
- the boundary conditions;
- the forces that are applied on it.

A good approximation of the structural shape and an estimate of materials distribution are generally achievable (Figure 1). Visual inspection, boreholes, and any available documentation are useful for the purpose.

The applied forces depend on the structure usage and can be prescribed, measured or controlled.

From the previous considerations, material parameters and boundary conditions are the most uncertain properties and may vary in time. It is the purpose of an identification tool to identify these properties. Once that the process has been completed, more reliable stress and safety analyses will follow.

2.2 The Finite Element Model

The process is based on the Finite Element model of the structure under consideration (Step 2). The geometry of the structure must be described in terms of a mesh (Figure 2). Critical issues are:

- the respect of the actual shape;
- an adequate mesh subdivision: usual validation criteria available in most mesh modellers can be used; an alternative is to subdivide into 5-10 elements the shortest wave length involved in the modal analysis;
- a proper definition of element groups sharing the same material properties, which will be involved in the model updating procedure; expected material distribution, potential fault locations as well as any location of interest to the engineer should be included;
- a realistic simulation of the boundary conditions applied on the structure.

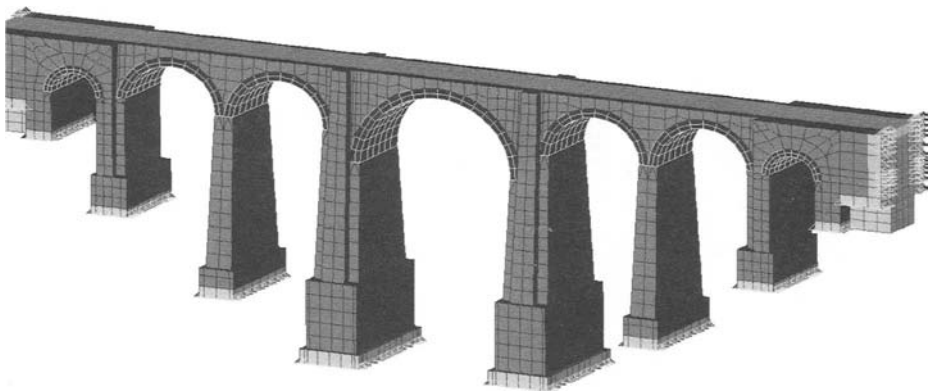


Figure 2. The 3D mesh of the masonry arch bridge used for identification: different material properties and boundary conditions are assigned.

2.3 Preliminary Modal Analyses

The identification approach is based on the comparison of the actual structure modal properties with those computed using the Finite Element model. Modal properties (a mode, in short) include frequencies, damping coefficients and modal shapes. Each mode depends on:

- the geometrical shape;
- the material properties;
- the boundary conditions.

If one assumes that geometry is known (and correctly meshed, as discussed in the previous step), it is possible to use modes to derive information on materials and boundary conditions.

The number of modes associated to any actual structure is theoretically infinite, whereas modes obtainable from the Finite Element model are as many as the model nodes. The identification process can use a few modes (up to some tenths, depending on the structure relevance, the available resources, etc.). The most significant modes must be selected adequately (Step 3) and the modal energy concept is used to this aim.

Each modal shape is indeed a deformation pattern and the related elastic energy indicates those parts more actively involved (i.e. having higher energy values, Figure 3). Conversely, a given mode depends on the activated parts and their material properties. It follows that if one includes at least one mode exhibiting high modal energy for each of the parts of concern, the best subset of modes is obtained.

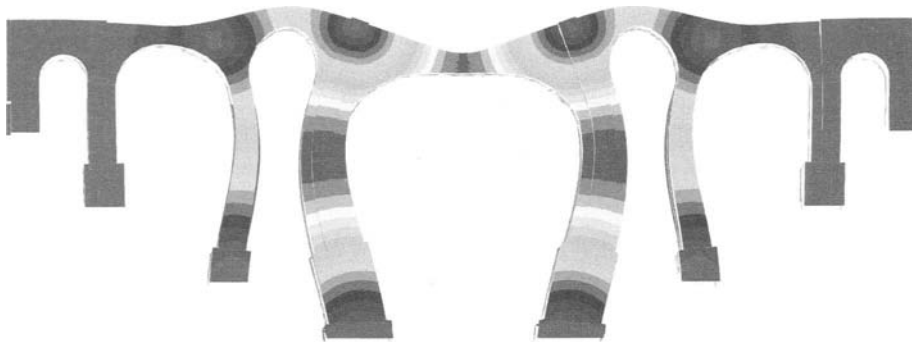


Figure 3. Contour representation of the elastic energy for one of the bridge modes.

2.4 Data Acquisition Planning

The quality of measured data is critical for a reliable identification. Yet, data capture on a structure is generally expensive and the number of available sensors is limited. As the quality of

measured data depends on the sensor locations it is important to optimise these locations to guarantee effective measurements (Step 4).

There exist many alternatives in evaluating the best locations: such as the Effective Independence Distribution Vector described by Magand et al., (2000), aiming to those measurement locations which make the mode shapes as linearly independent as possible. This planning module can be fully based on the numerical Finite Element model. Trial and error procedures based on the real structure are completely eliminated, dramatically reducing costs and improving efficiency.

2.5 Testing the Structure

The aim of the Step 5 is to apply sensors in the optimal positions previously defined and to measure the dynamic responses while the structure is vibrating. The success of the experimental measurements is achieved if data are significant, i.e. statistically stable and representative of a structural state. Lessons learnt from past experiences are very useful.

Response can be measured in terms of acceleration (velocity or displacement) vs. time, depending on the sensors available, the frequency range, the amplitude of vibrations, etc.

Velocity measurements are to be preferred for low frequency structures (first frequency below 1 Hz, up to 10-20 Hz), whereas accelerometer can be more convenient for higher frequency bands (more than 20-30 Hz). Relative displacements transducers are generally used across cracks and joints. Raw data may be stored in analogue or digital formats.

Excitation of the structure can be obtained in some alternative ways, depending on the resources available, the structure relevance and the testing purpose.

The more expensive and reliable solution is to apply one (or more) excitors on the structure (unbalanced rotating mass, hydraulic piston, etc.). The excitors can be conveniently controlled in terms of frequencies and amplitudes. All the structural resonance within the available excitors frequency working range will be clearly activated. This approach is strongly recommended for massive structure.

A much cheaper excitation source is represented by environmental vibrations as induced by urban traffic, wind etc. In this case signals are corrupted and long acquisition times must be planned so to perform many averages to remove noise. Good results can be achieved for slender tall structures (towers, chimneys, bridges, etc.).

Two more alternatives are the pull & release test and the impact test. The former is very good to induce free decay transients which are convenient to measure damping behaviours. Signals are generally good, even if short in time. Some safety problems may arise when the steel wire is released.

The latter is used in the case of non massive structures (mechanical components, steel members, etc.) and also to test structural details (concrete slabs, junctions, etc.). If it is performed using an instrumented hammer, the input force is known. The test is easily repeatable varying the force amplitude and location.

All of the above tests must be properly selected and performed not to induce any damage on the structure itself. It is recommended to compare the expected (and acceptable) amplitudes of vibration as computed on the model with those measured on the real structure. Also, a real time control on the data quality must be carried out (null or saturated signals must be avoided, etc.).

2.5 Experimental Modal Analyses

It is the purpose of this phase to derive experimental modal features from the dynamic measured responses (Step 6). Raw data are the time histories as measured from each sensor for all the different testing conditions (Figure 4).

A preliminary control on the data quality must be carried out (null or saturated signals must be removed, etc.). Also, it is recommended to compute some Fourier Transform on sample data to check the frequency content of the signals. Undesired (or clearly unphysical) frequencies can be removed by filtering. Expected structural resonance can be broadly checked, as well as varying frequency values during testing can be appreciated using time-frequency analysis.

Next step is the computation of modal features, evaluating Transfer Functions (Figure 5), using for instance the State Space algorithm as described by Magand, (2000). This method is applicable on any time signals, providing a general purpose and up-to-date tool for extracting modal features. Real and Imaginary components of frequencies and shapes are obtained without any approximation. There is no limitation either on the number of sensors or on the signal samples. Frequencies can be sorted by statistical relevance as well as it is possible to compare the original data with those synthesized numerically using the modal identified features.

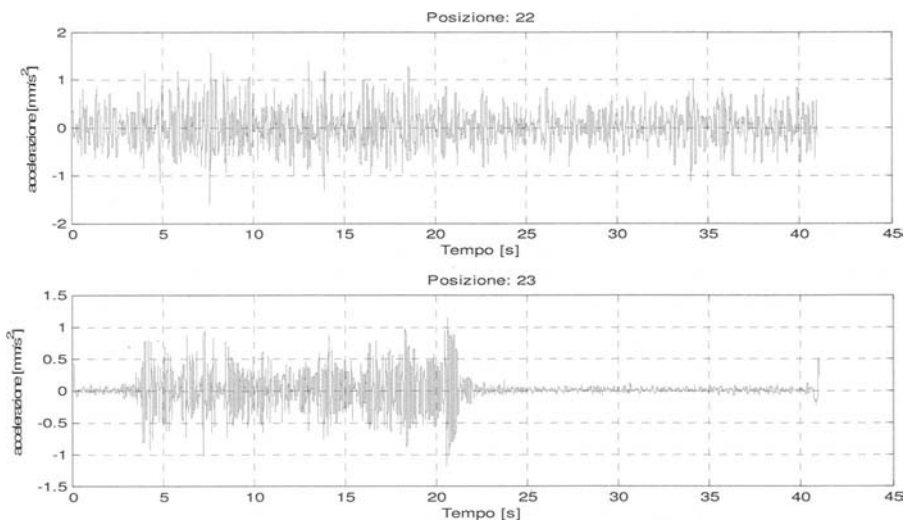


Figure 4. Typical acceleration time histories as obtained from two different train motions (axes scale are mm/s^2 and s).

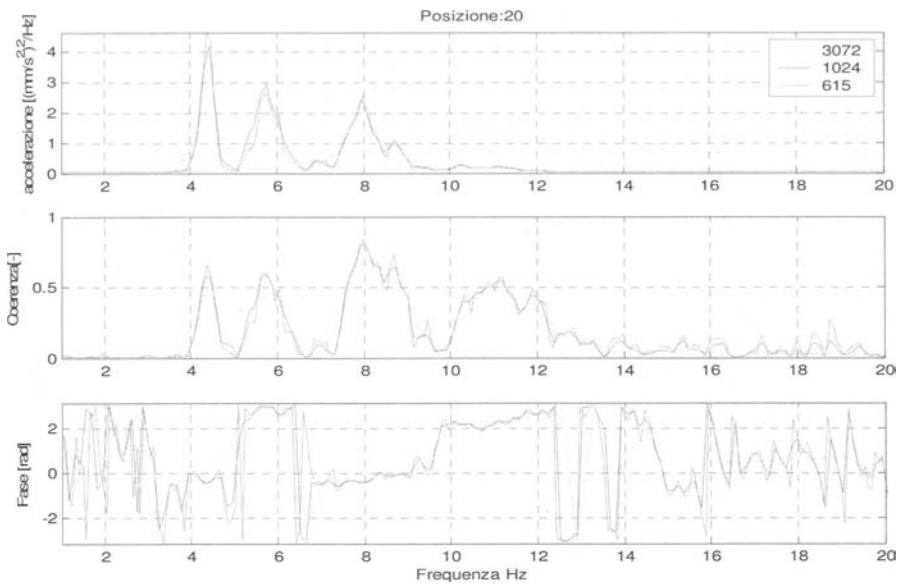


Figure 5. An example of experimental pseudo-transfer function. From top: amplitude, coherence, and phase for different averaging of signal (horizontal axis scale is Hz).

Some specific time signals can be successfully used for further insights and to evaluate, for instance, damping coefficients or crack relative movements. In the former case the Hilbert Transform (Figur 6) can be used to compute the damping related to a structural frequency as shown by Bolognini, Galimberti, Meghella, (1995).

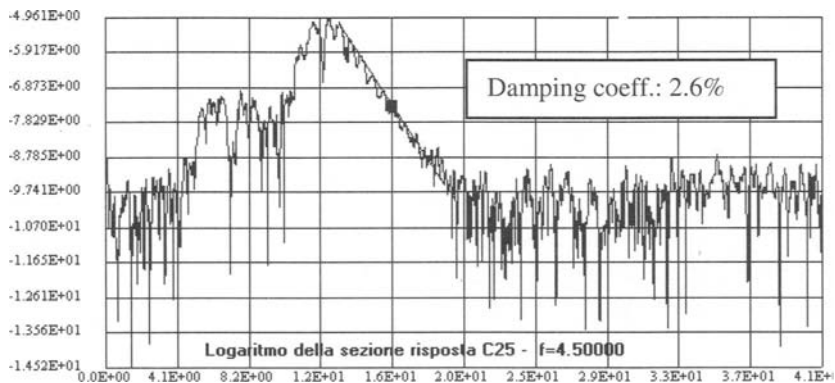


Figure 6. A free decay envelope in the log-axis, for the approximation of damping coefficient via Hilbert Transform.

2.6 Modal matching / model updating

The difference between experimental modal features and the corresponding numerical ones are minimised by an iterative correction of those physical parameters affecting the solution (Step 7).

Modal features involved in the process can be both real and imaginary parts of frequencies and shapes. Thus, to generalize the classic modal identification approach, one has to manage a full complex modal analysis, both experimental and numerical (§ 3.1). A general damping matrix is explicitly included in the numerical eigenvalue problem as described in Chapter 4, removing previous limitations to the modal damping modelling (bridge spans with dampers, for instance, are a new potentiality offered); coupled 3D fluid structure problems can be analysed as well as discussed by Brusa, (1999).

The process is based on the computation of the derivatives (sensitivities) of all modal quantities with respect to each parameter and the solution of a constrained least squares problem. In the following the basic formulation is described, whereas the general approach is presented in Chapter 3.

Basic formulation. The described identification method searches for the minimum distance between vector \underline{Y}^m containing experimental eigenvalues and eigenshapes and vector $\underline{Y}^e(\underline{p})$ where the corresponding quantities are stored as obtained numerically, being $\underline{Y}^e(\underline{p})$ function of L parameters p_i , multipliers of "initial guess" structural parameters.

These parameters are related to L sets of finite elements sharing the same parameter ("macroblocks") defined on the structure and they are supposed to be coefficients of the linear combination which relates the related matrix of the whole structure. Defining the difference vector \underline{b} and its norm $d(\underline{p})$ as a distance between the two aforesaid vectors:

$$\underline{b} = \underline{Y}^e(\underline{p}) - \underline{Y}^m; \quad d(\underline{p}) = \underline{b}^T(\underline{p}) \mathbf{W}^T \mathbf{W} \underline{b}(\underline{p}) \quad (2.1.a, 2.1.b)$$

$$\underline{b}^T(\underline{p}) \mathbf{W}^T \mathbf{W} \frac{\partial \underline{b}(\underline{p})}{\partial \underline{p}} = 0 \quad (2.2)$$

being $\mathbf{W}^T \mathbf{W}$ a weight matrix, symmetric positive definite, the necessary condition for the minimum of the norm $d(\underline{p})$ can be stated as:

Introducing a linear approximation for vector $\underline{b}(\underline{p})$ by the Taylor's expansion up to first order terms, a Least Squares iterative procedure derives from Equation (2.2), that is:

$$\mathbf{S}_j^T \mathbf{W}^T \mathbf{W} (\mathbf{S}_j \Delta \underline{p}_{j+1} - \underline{b}_j) = 0 \quad (2.3)$$

$$\text{where } \mathbf{S}_j = \mathbf{S}_j(\underline{p}) = [\partial \underline{Y}^e / \partial p^1, \dots, \partial \underline{Y}^e / \partial p^L]_j$$

where \mathbf{S}_j and \underline{b}_j indicate respectively sensitivity matrix and residual vector as calculated in the j -th iteration, whilst Δp_{j+1} means the new variation of parameters ($p_{j+1} = p_j - \Delta p_{j+1}$; $p_0 = 1$).

The iterative procedure defined by Equations (2.3) ends when a new iteration is unable to reduce either parameters variation or residual norm given below a given tolerance. Starting from results obtained according to the given initial values of parameters and from available experimental data, the identification procedure runs iteratively to the best approximation of the parameters.

3 Extended Set of Identification Parameters

The typical version of a modal identification tool is able to manage only those parameters which affects merely the stiffness matrix K (and/or mass matrix M).

This limitation is due to the fact that the eigenvalue problem is solved under the hypothesis that the damping matrix C is negligible or proportional to K and M .

The extended identification method introduces a substantial enhancement with respect to the above identification, allowing the user to choose among an extended set of parameters. The idea is that free parameters (i.e. subject to modification) may affect respectively the stiffness matrix K , the mass matrix M and the damping matrix C , explicitly included in the standard eigenvalue equation (3.4) of Paragraph 3.1.

The case of a single parameter affecting more than one matrix simultaneously can be taken into account as well.

The general formulation of Finite Element theory asserts that if the calculation domain is subdivided in N zones having different properties (either physical or geometrical) described by a parameter p , the following relations hold:

$$K = \sum_{i=1}^N K_i(p_i) \quad M = \sum_{i=1}^N M_i(p_i) \quad C = \sum_{i=1}^N C_i(p_i) \quad (3.1)$$

where summation means matrices assembly and where K_j , M_j and C_j are zone matrices.

According to the proposed method, it is required that, if the stiffness matrix K is considered (but the same procedure could be applied to M and C as well), the dependency on the parameter is of the kind:

$$K = \sum_{i=1}^N K_i(p_i) = \sum_{i=1}^N (p_i A_i + B_i) \quad (3.2)$$

being A_j and B_j not dependent on p .

This hypothesis is necessary in order to compute the first derivative of a matrix with respect to the parameter without knowing all the physical and geometry data used in its formulation:

$$\frac{\partial K}{\partial p_i} = A_i \quad (3.3)$$

3.1 Reduction of the eigenvalue problem to standard form

In this section the generalized eigenvalue problem is considered. Afterwards, by distinguishing two particular cases (damped/undamped), the explicit expressions of the corresponding standard form are derived. More details and the discussion of coupled fluid-structures complex cases can be found in Brusa L., (1999).

The following generalized eigenvalue problem is considered:

$$\tilde{K}Z + \lambda \tilde{C}Z + \lambda^2 \tilde{M}Z = 0 \quad (3.4)$$

where \tilde{K} , \tilde{C} , \tilde{M} is a given set of $n \times n$ matrices, λ is a scalar and Z is a n components vector. The problem (3.4) is equivalent to the following standard problem:

$$A\Phi = \lambda\Phi \quad (3.5)$$

where:

$$A = \begin{vmatrix} 0 & I \\ -\tilde{M}^{-1}\tilde{K} & -\tilde{M}^{-1}\tilde{C} \end{vmatrix}; \quad \Phi = \begin{vmatrix} Z \\ \lambda Z \end{vmatrix} \quad (3.6)$$

If it is possible to find a matrix Γ such that:

$$A^T = \Gamma A \Gamma^{-1} \quad (3.7)$$

then each of the $r = 2n$ “left eigenvector” Ψ_k of matrix A^T , solution of the problem:

$$A^T \Psi_k = \lambda_k \Psi_k \quad (3.8)$$

can be related to the “right eigenvector” Φ_k , solution of the problem (3.5), by the equation:

$$\Psi_k = \Gamma \Phi_k \quad (3.9)$$

Therefore, since Ψ_k and Φ_k are orthogonal by definition, the following ortho-normalization condition can be assumed:

$$\Phi_k^T \Gamma \Phi_j = \delta_{kj} \quad (3.10)$$

where $k, j = 1, \dots, r$ and δ_{kj} means the Kronecker symbol. The explicit form of the standard problem (3.5,6) together with relation (3.10) can be useful for computing the derivatives of eigenvectors and eigenvalues with respect to a parameter. Moreover, in doing derivative algebra, it is valuable requiring Γ to be a symmetric matrix.

Undamped structural problem (real eigenvectors and eigenvalues). Problem (3.4) specialised for the undamped structural eigenvalue problem reads:

$$M^{-1}KZ = \mu Z; \quad \mu > 0 \quad (3.11)$$

where M is the mass matrix and K is the stiffness matrix of the structural system. The problem (3.11) is equivalent to the following standard problem:

$$A\Phi = \mu\Phi; \quad \text{with: } A = -M^{-1}K \quad \text{and} \quad \Phi = Z \quad (3.12)$$

By choosing, $\Gamma = K$ relation (3.7) is satisfied and the ortho-normalization condition (3.10) is:

$$Z_k^T K Z_j = \delta_{kj} \quad (3.13)$$

Damped structural problem (complex eigenvalues and eigenvectors). Problem (3.4) specialised for the damped structural eigenvalue problem reads:

$$-M^{-1}KZ - \lambda M^{-1}CZ = \lambda^2 Z \quad (3.14)$$

where M is the mass matrix, C is the damping matrix and K is the stiffness matrix of the structural system. The problem is equivalent to the standard problem $A\Phi = \lambda\Phi$ with:

$$A = \begin{vmatrix} 0 & I \\ -M^{-1}K & -M^{-1}C \end{vmatrix} \quad \Phi = \begin{vmatrix} Z \\ \lambda Z \end{vmatrix} \quad (3.15)$$

By choosing:

$$\Gamma = \begin{vmatrix} 0 & K \\ K & C \end{vmatrix} \quad (3.16)$$

the relation (3.7) is satisfied and the ortho-normalization condition (3.10) is:

$$Z_k^T [(\lambda_k + \lambda_j)K + \lambda_k \lambda_j C] Z_j = \delta_{kj} \quad (3.17)$$

3.2 First derivatives of the eigenvectors and eigenvalues with respect to a parameter

Let us consider the standard eigenvalue problem (3.5), with $\Gamma = \Gamma^T$ such that:

$$A^T = \Gamma A \Gamma^{-1} \quad (3.18)$$

and with the normalisation condition:

$$\Phi_k^T \Gamma \Phi_j = \delta_{kj} \quad (3.19)$$

If matrix A depends on a parameter p , the derivatives of the eigenvectors with respect to this parameter, being vectors of the space generated by the eigenvector system itself, are computed with the following formal expansion:

$$\frac{\partial \Phi_j}{\partial p} = \sum_k c_k^{(j)} \Phi_k; \quad \text{with: } c_k^{(j)} = \Phi_k^T \Gamma \frac{\partial \Phi_j}{\partial p} \quad (3.20)$$

It should be noted that the complete set of eigenvectors Φ_k might include pairs of conjugate complex vectors, if complex eigenvalues exist. Therefore, in this case, equation (3.20) can be explicitly written in the following form:

$$\frac{\partial \Phi_j}{\partial p} = \sum_k (c_k^{(j)} \Phi_k + \tilde{c}_k^{(j)} \bar{\Phi}_k); \quad \text{with: } c_k^{(j)} = \Phi_k^T \Gamma \frac{\partial \Phi_j}{\partial p}; \quad \tilde{c}_k^{(j)} = \bar{\Phi}_k^T \Gamma \frac{\partial \Phi_j}{\partial p} \quad (3.21)$$

where the bar over a variable indicates its conjugate complex value.

The derivatives of the eigenvectors with respect to this parameter are computed with the following expansion equivalent to the relation (3.21):

$$\frac{\partial \Phi}{\partial p} = \Phi S + \bar{\Phi} \tilde{S} \quad \text{with: } S = \Phi^T \Gamma \frac{\partial \Phi}{\partial p}; \quad \tilde{S} = \bar{\Phi}^T \Gamma \frac{\partial \Phi}{\partial p} \quad (3.22)$$

With reference to the relation (3.21), the elements of matrices are respectively:

$$S_{kj} = c_k^{(j)} \quad \text{and} \quad \tilde{S}_{kj} = \tilde{c}_k^{(j)} \quad (3.23)$$

As shown by Brusa, Bolognini, (1999) the coefficient of matrices S, \tilde{S} and the derivatives of the eigenvalues can be computed.

4 A General Damping Model

The interest for a general damping model comes from the need of analysing a wide variety of structural components, such as point dampers in bridges, or dissipative devices in mechanical components.

Yet, it must be emphasized that the importance of simulating a general damping behaviour is very often dictated by the experimental outcomes. Figure 7 is the polar plot of the vectors representing an experimental modal shape of a dam, as discussed by Bolognini, Frigerio, (2001). The Real Axis (depicted in red) is the expected locations of modal values in the case of undamped or proportionally damped behaviours, whereas the blue points are the actual experimental values. It can be seen that most of the points are averagely $\pm 30^\circ$ out of the red line, exhibiting a relevant Imaginary component (vertical axis). The usual practice is to project the blue points on to the Real Axis, introducing an unrealistic approximation since the beginning of the identification process.

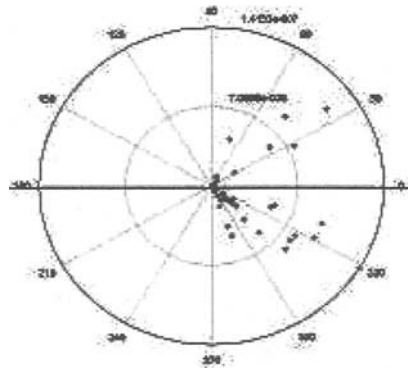


Figure 6. Polar plot of vectors representing an experimental modal shape.

4.1 Non-Proportional Damping Model

If a general structural eigenvalue problem is considered of the form:

$$KZ + \lambda CZ + \lambda^2 MZ = 0 \quad (4.1)$$

depending on the form of matrix C , both real and complex eigensolutions can be found. A necessary and sufficient requisite in order to force the solution of the corresponding standard problem to be complex, is that C expresses a condition of non-proportional damping. This means, by using the definition of proportional damping, requiring that the C matrix is such that:

$$\Pi = CM^{-1}K \quad (4.2)$$

is strictly non symmetric. As a counter example, the well known Rayleigh damping matrix, defined as:

$$C = \alpha K + \beta M \quad (4.3)$$

does not satisfy (4.2), since:

$$\Pi = CM^{-1}K = (\alpha K + \beta M)M^{-1}K = \alpha KM^{-1}K + \beta K \quad (4.4)$$

is symmetric because of the symmetry of both K and $KM^{-1}K$:

$$(KM^{-1}K)^T = K^T M^{-T} K^T = KM^{-1}K \quad (4.5)$$

In what follows, we show two possible way of choosing C such as condition (4.2) is satisfied.

4.2 A Rayleigh damping model depending on element zones

A first method to loose the proportionality is to define local α_i and β_i Rayleigh coefficients not globally over the whole structure, but related to the N element zones which compose the structure. In this case for any possible choice of global α and β we have:

$$C = \sum_{i=1}^N C_i = \sum_{i=1}^N (\alpha_i K_i + \beta_i M_i) \neq (\alpha K + \beta M) \quad (4.6)$$

In this way the validity of (3.2) does not hold, because:

$$\Pi = CM^{-1}K = \sum_{i=1}^N (\alpha_i K_i M^{-1}K + \beta_i M_i M^{-1}K) \quad (4.7)$$

and the members of the sum are symmetric only in the trivial case $N=1$. That would mean the Rayleigh damping again.

4.3 A damping model using "damper" elements

Another possible approach is the use of "damper" elements, for which the element damping symmetric matrix can be defined as:

$$C^e = \begin{pmatrix} \gamma_{1,1} & \gamma_{1,2} & \cdots & \gamma_{1,n} \\ \gamma_{2,1} & \gamma_{2,2} & \cdots & \gamma_{2,n} \\ \cdots & \cdots & \cdots & \cdots \\ \gamma_{n,1} & \gamma_{n,2} & \cdots & \gamma_{n,n} \end{pmatrix} \quad \text{where} \quad \gamma_{i,j} = \gamma_{j,i} \quad (4.8)$$

and n is the number of element degrees of freedom. Also in this case, apart from the trivial case $C^e = K^e \forall e \Leftrightarrow C=K$ the symmetry fails, leading to a non-proportionally damped system. This is very useful to manage point dampers, such as in the case of bridge deck supports, which have a huge impact on seismic safety evaluations.

5 The Identification Process

As previously stated, one of the aim of identification is to provide realistic models of structures in their current state. These models can be used for safety evaluations strongly improved and reliable. This is indeed the outcome of many industrial cases, whose divulgation is obviously restricted.

The difference between an identified model and the “prior” model are presented by Bolognini, Frigerio, (2001), and by Bolognini, Galimberti, (1995) with reference to dams. Two examples are given in the following Tables 1 and 2: the effect of identification can be clearly understood.

Table 1. “Prior “ model, experimental and identified values of five vibrating frequencies of a dam.

NUMERICAL values (before identification)		EXPERIMENTAL values		NUMERICAL values (after identification)	
Real part	Imaginary part	Real part	Imaginary part	Real part	Imaginary part
-0.5916E+00	0.4439E+02	-0.1027E+01	0.5706E+02	-0.1345E+01	0.5655E+02
-0.1624E+01	0.7356E+02	-0.1664E+01	0.7567E+02	-0.2013E+01	0.7711E+02
-0.2018E+01	0.8200E+02	-0.1902E+01	0.8648E+02	-0.2303E+01	0.8597E+02
-0.3430E+01	0.1069E+03	-0.2455E+01	0.1023E+03	-0.2634E+01	0.1001E+03
-0.3041E+01	0.1235E+03	-0.2687E+01	0.1222E+03	-0.2854E+00	0.1260E+03

Table 2. Seismic analysis: some results from the “prior” model (M1) and the identified one (M2).

	Displacement 10^{-4} [m]			Acceleration [m/s ²]			Normal Stress 10^5 [Pa]			Tangential Stress 10^5 [Pa]		
	S_x	S_y	S_z	A_x	A_y	A_z	σ_x	σ_y	σ_z	τ_{xy}	τ_{yz}	τ_{zx}
M1	5.8	4.3	2.1	2.2	1.6	1.0	2.2	3.6	2.3	1.4	1.8	1.7
M2	4.0	2.3	1.3	2.3	1.3	0.8	1.6	2.6	2.4	.74	.99	.88

6 Open Issues and Further Enhancements

It is important to remember that identification is an inverse problem: this induces some peculiarities if compared with the usual problems of design and verification, as discussed in Bolognini et al., (2001).

- The solution may be not unique; there exist more than one combination leading to the same result. Always check feasibility of solutions and use engineering judgement.
- Experimental modal shapes are noisy data and related to few locations: interpolations tend to be arbitrary and unreliable.
- The objective function should be complete: all the parameters (and not more) affecting the selected eigensolutions Y should be included;
- The objective function should be significative: all the eigensolutions which are necessary for the description in the space of the selected variables of the actual problem have been included.
- Static measurements can be included to reduce feasibility space of unknown parameters.
- Modal identification can be unstable: to compute the modal error, you must assign to any experimental modes the nearest computed one, according to $\|\Psi E_i - \Psi C_j\|_{MAC} \leq \|\Psi E_i - \Psi C_j\|_{MAC}$. When updating parameters a mode never considered before can become nearer (to a given experimental one) than any previously selected. To overcome this problem the Objective Function approach is being studied.
- Other approaches could be more robust: static or dynamic, in time domain.
- Up-to-date minimisation algorithm could be used: combinatory solvers (genetic, for instance).
- New measurement techniques are at hand: optical fibers, laser and radar.
- Use identification techniques aiming to the modelling of behaviours and not to the understanding of causes (Quadratic and Narma-X, Neural Networks, Fuzzy Logic, etc..).

In the end, models and reality will be getting closer.

References

- Magand F. et al., (2000). Data Acquisition Planning Module Specifications. HISTRIDE ESPRIT Project 28249, Deliverable D4.4.1.
- Magand F., (2000). Application d'une méthode temporelle d'estimation de modes propres (fréquences et amortissements) par sous-structuration dans l'espace d'états. ASTELAB Symposium (6th International Testing Laboratory Exhibition), Paris.
- Bolognini L., Galimberti C., Meghella M., (1995). Identification of Dynamic Response of Structures. Proceedings of the 13th IMAC, Nashville.
- Brusa L., (1999). Strategy for Complex Eigensolutions. HISTRIDE ESPRIT Project 28249, Deliverable D4.1.1.
- Brusa L., Bolognini L. (1999). Enhanced Modal Matching. HISTRIDE ESPRIT Project 28249, Deliverable D4.2.1.
- Bolognini L., Frigerio A., (2001). Dam Case Study. HISTRIDE ESPRIT Project 28249, Deliverable D6.5.1.
- Bolognini L., Galimberti C., (1995). Identificazione strutturale e credibilità delle verifiche sismiche: applicazione ad una diga ad arco. Atti del 7° Convegno Nazionale ANIDIS L'ingegneria Sismica in Italia, Siena 25-28/IX/95.
- Bolognini L. et al., (2001). Final Integrated Report. HISTRIDE ESPRIT Project 28249 FP.

The Reciprocity Gap Functional for Identifying Defects and Cracks

H.D. Bui, A. Constantinescu and H. Maigre

Laboratoire de Mécanique des Solides, CNRS,
Ecole Polytechnique, Palaiseau, France

Abstract. The recovery of defects and cracks in solids using overdetermined boundary data, both the Dirichlet and the Neumann types, is considered in this paper. A review of the method for solving these inverse problems is given, focusing particularly on linearized inverse problems. It is shown how the reciprocity gap functional can solve nonlinear inverse problems involving identification of cracks and distributed defects in bounded solids. Exact solutions for planar cracks in 3D solids are given for static elasticity, heat diffusion and transient acoustics.

1. Introduction and Scope

There are many classes of inverse problems for detection of defects in solids: recovery of distributed coefficients, densities, identification of cavities and cracks.

The recovery of coefficients or densities in a domain from line integrals, known as “Ray Tomography”, with X-rays or Gamma-rays, single or double photon emission... is possible owing, on the one hand, to highly sophisticated data acquisition systems such as Scanners, Photonic Collimators and, on the other hand, to mathematical techniques like the Radon transform and its exact inverse, with or without absorption. The case of Gamma ray tomography, taking account of the Compton electron diffusion, has been investigated recently by Nguyen and Truong (2002) and Nguyen et al (2002) who gave the exact inverse of the so-called “Conical Radon Transform”. For optical absorption and scattering tomography, the

mathematical models are given by the Boltzmann transport equation and the diffusion equation. For a review of the topic, see Arridge (1999).

Applications of acoustics in geophysics and non destructive testing of materials are based on mechanical set-ups like the transducers which collect data on their boundary. Mathematically one deals here with inverse scattering theories which are based on some approximations: incident plane waves, Born's approximation, Kirchhoff's approximation (see Bui, 1993, 1994). Analytical solutions exist only for some specific problems. For example, in "Acoustics tomography", under the above approximations, an exact solution to the inverse scattering of a rigid inclusion has been given by Bojarski (1981). The classical "Elastic Wave Tomography" using the Kirchhoff approximation, the far-field analysis and the assumption of smallness of the defects, leads to the so-called POFFIS method (Physical Optics Far Field Inverse Scattering). Most works applied to Geophysics are generally based on numerical methods such as Finite Elements Method, Boundary Integral Equations, Optimal Control theory (Lions, 1971).

Recently a large amount of work has been devoted to "Generalized Tomography" applied to different physical phenomena ranging from elliptic to parabolic and hyperbolic equations. Such works are yet at the stage of primary developments of methods for computational and for pure and applied mathematical purposes. Despite the existence of new devices such as the Infra-Red camera already used for investigation of delaminations in composites structures or functional observations in Biology, its industrial applications are not well developed. One explanation is the lack of exact solutions to thermal inverse problems which can be used as a benchmark for computational solutions and, above all, the difficulties encountered in numerical methods for ill-posed inverse problems.

The aim of this paper is to review some recent works done in the applied mathematics for identifying defects in solids. It focuses mainly on the following topics:

- a. Derivation of the "Observation Equation" using the notion of "Defect Indicators".
- b. General considerations on non-linear and linearized inverse problems.
- c. Linear inverse problems settings; Ill-posedness; Regularizations methods; Mathematical aspects; The Cauchy Problem.
- d. Exact solutions of the inverse problems for identifying a planar crack in the 3D case, for elliptic, parabolic and hyperbolic equations, from overdetermined boundary data.

2. Defects and cracks indicators

The boundary data for recovering the defects provides qualitative and quantitative informations about the unknowns by means of defect indicators. If there exists a relationship between the boundary data and the parameters which characterizes the unknown defects, this relationship can be used as a defect indicator. Generally the indicator is a boundary integral which vanishes in the case of absence of defect or relates to the strength of the singularities inside the body, the location of point forces, or the crack geometry, etc.

The method for obtaining indicators are based on conservation laws which transfer the information about the mechanical field inside the body to the exterior boundary S where boundary data can be obtained, without solving any boundary value problem. Let us consider

some types of indicators in the following examples. Consider a first class of indicator defined by a conservation law of the form $-\text{div}(\mathbf{A})=\mathbf{B}$ in Ω , with \mathbf{B} a source term.

The defect indicator is given by the boundary integral

$$I = - \int_S \mathbf{A} \cdot \mathbf{n} \, dS \quad (1)$$

over the exterior surface S of the body. The integral (1) vanishes (or not) if $\mathbf{B}=0$ (or $\mathbf{B} \neq 0$), indicating the absence (or presence) of the source. As an example, consider the stress field $\sigma(\mathbf{x})$ in a 3D solid,

$$-\text{div}\sigma(\mathbf{x}) = \mathbf{f}\delta(\mathbf{x}-\mathbf{a}) \quad \text{in } \Omega \quad (2)$$

with the point force $\mathbf{f}\delta(\mathbf{x}-\mathbf{a})$. The integral (1) is equal to the total force \mathbf{f} .

Consider another class of indicator more general than (1), in the case of linear elasticity under small strain. Denote by $\sigma[\mathbf{u}](\mathbf{x})$ the stress field corresponding to the displacement field $\mathbf{u}(\mathbf{x})$ in the solid due to the point force $\mathbf{f}\delta(\mathbf{x}-\mathbf{a})$. Introduce an auxiliary field $\sigma[\mathbf{v}](\mathbf{x})$ associated to the displacement field $\mathbf{v}(\mathbf{x})$, without body force. We get

$$-\text{div}\{\sigma[\mathbf{u}]\cdot\mathbf{v} - \sigma[\mathbf{v}]\cdot\mathbf{u}\} = \mathbf{v} \cdot \mathbf{f} \delta(\mathbf{x}-\mathbf{a}) \quad \text{in } \Omega \quad (3)$$

The indicator derived from (3) is the linear form $\mathbf{v} \rightarrow I(\mathbf{v})$

$$I(\mathbf{v}) = - \int_S \{\mathbf{n} \cdot \sigma[\mathbf{u}]\cdot\mathbf{v} - \mathbf{n} \cdot \sigma[\mathbf{v}]\cdot\mathbf{u}\} dS \quad (4)$$

which contains the information on both the force \mathbf{f} and the point \mathbf{a} .

This indicator is twice the bilinear symplectic form corresponding to the energy release rate in linear Fracture Mechanics.

Exercices. Take $\mathbf{v}=(v_j)$, $v_j=\delta_{ij}$ and verify that $I(v_j)=f_i$.
Take $\mathbf{v}=(v_j)$, $v_j=x_k\delta_{ij}$ and verify that $I(v_j)=a_k f_i$. ♦

2.1. Crack indicator

Let us introduce another class of indicators more suitable for crack detection. We assume that the stress field $\sigma[\mathbf{u}](\mathbf{x})$ corresponds to the stress field of the previous 3D elastic solid with an unique internal crack Σ , with some boundary conditions on S and without body force. We assume that $\mathbf{v}(\mathbf{x})$ corresponds to the auxiliary (or adjoint) field of the *uncracked* solid, with the same elastic constants and some different boundary conditions. The indicator given by (4) is called here the Reciprocity gap $R(\mathbf{v})$

$$R(\mathbf{v}) = \int_S \{\mathbf{n} \cdot \sigma[\mathbf{v}]\cdot\mathbf{u} - \mathbf{n} \cdot \sigma[\mathbf{u}]\cdot\mathbf{v}\} dS \quad (5)$$

The reason of the word "gap" in the name comes from the fact that in an uncracked body, the Betti reciprocity relation yields $R(\mathbf{v})=0$, for any \mathbf{v} satisfying the elasticity equation. Hence a non vanishing value of $R(\mathbf{v})$ indicates the presence of a crack. More precisely by introducing the displacement jump defined as $[[\mathbf{u}]] = \mathbf{u}^+ - \mathbf{u}^-$ one gets

$$R(\mathbf{v}) = \int_{\Sigma} \mathbf{n} \cdot \boldsymbol{\sigma}[\mathbf{v}] \cdot [[\mathbf{u}]] dS \quad (6)$$

where $\mathbf{n} = \mathbf{n}^- = -\mathbf{n}^+$. From (5) and (6) one obtains the "observation equation"

$$\int_{\Sigma} \mathbf{n} \cdot \boldsymbol{\sigma}[\mathbf{v}] \cdot [[\mathbf{u}]] dS = \int_S \{ \mathbf{n} \cdot \boldsymbol{\sigma}[\mathbf{v}] \cdot \mathbf{u} - \mathbf{n} \cdot \boldsymbol{\sigma}[\mathbf{u}] \cdot \mathbf{v} \} dS \quad (7)$$

Equation (7) has been derived in many works as a tool for crack identification. It can be generalized to transient problems in elasticity, acoustics, and also to heat diffusion problems (See Section 7.2). The use of (7) for crack identification using an overdetermined boundary data pair $(\mathbf{u}, \mathbf{T} := \mathbf{n} \cdot \boldsymbol{\sigma}[\mathbf{u}])$ will be discussed in Section 7. Let us remark that Equation (7) alone is not sufficient for identifying the crack Σ . We shall discuss further two important questions : the number of data pairs (\mathbf{u}, \mathbf{T}) and the nature of adjoint fields which are necessary and sufficient for a complete identification. The identifiability question is important because it is related to *uniqueness* of the solution of the inverse problem for *exact* data pair. In contrast with the identifiability problem, practical solutions to crack or defect inverse problems are based on numerical computations which generally make use of *noise-contaminated* data pairs. In this case, the key issues are the continuity of approximate solutions with respect to data variation and an error estimate with respect to the exact solution. These questions will be examined for linear inverse problems which are simpler than nonlinear inverse problems.

2.2. Distributed Defect Indicator

The following example is given by Calderon (1980) for transient as well as for static heat diffusion equation. Let us restrict to the static case. Distributed defects in solids are due for example to the presence of microscopic voids and micro-cracks which change macroscopically the thermal diffusion coefficient, from the known constant value k_0 to $k(\mathbf{x}) = k_0 + c(\mathbf{x})$.

Without loss of generality, we consider normalized constant so that $k_0 = 1$ and assume that $c(\mathbf{x}) = 0$ on $\partial\Omega$. In the macroscopic scale, $c(\mathbf{x})$ can be considered as the damage field.

The inverse problem consists of finding $c(\mathbf{x})$ from measurements of surface temperature θ and temperature gradient $\partial_n \theta$.

The equations are the following ones.

–Actual field θ (damaged solid) :

$$- \operatorname{div}\{(1+c)\operatorname{grad} \theta\} = 0 \quad (\text{in } \Omega) \quad (8)$$

$$\partial_n \theta(\mathbf{x}) = f(\mathbf{x}) \quad (\text{on } \partial\Omega) \quad (9)$$

–Adjoint field ψ (undamaged solid):

$$-\operatorname{divgrad} \psi = 0 \quad (\text{in } \Omega) \tag{10}$$

$$\partial_n \psi(\mathbf{x}) = g(\mathbf{x}) \quad (\text{on } \partial\Omega) \tag{11}$$

The observation equation is given by :

$$\int_{\Omega} c \operatorname{grad}\theta[c] \cdot \operatorname{grad}\psi \, dV = \int_{\partial\Omega} \{\psi \partial_n \theta - \theta \partial_n \psi\} dS \quad (\equiv d) \tag{12}$$

The explicit dependence of $\theta[c]$ on c in Equation (12) and the solution of (8) and (9) under the compatibility condition $\int_{\partial\Omega} f dS=0$ clearly show that the observation equation is *nonlinear* with respect to c .

The observation equation (12) alone does not allow the determination of the scalar field $c(\mathbf{x})$ since its right hand side is a scalar constant denoted by d , for a given surface data pair $(\theta, \partial_n \theta)$ and for a given adjoint field $\psi(\mathbf{x})$. It is necessary to establish an one-to-one mapping between $c(\mathbf{x})$ and a larger family of data $d(\zeta)$ depending on some family of boundary data or of adjoint fields indexed by some N -dimensional parameter ζ .

To illustrate the necessary condition, suppose for example that $c(\mathbf{x})$ is a constant c inside a 2D ellipsoidal inclusion, and is equal to zero outside the inclusion, Figure 1. To determine the constant c and the ellipsoidal geometry, e.g. 6 unknown parameters (the constant c , 2 coordinates of the center, the orientation of the main axis, the semi axes a and b), many procedures can be used. One can consider a single data pair $(\theta, \partial_n \theta)$ measured on $\partial\Omega$ and six adjoint fields, or two data pairs $(\theta^1, \partial_n \theta^1)$, $(\theta^2, \partial_n \theta^2)$ and three adjoint fields etc. These conditions are necessary but not sufficient for solving the nonlinear inverse problem.

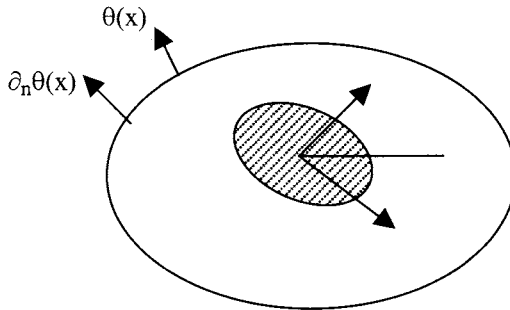


Figure 1. Two dimensional ellipsoidal inclusion.

Calderon (1980) proposed a linearization of (12) in order to obtain a simpler inverse problem, which can be solved exactly for 3D defects. His basic idea is the consideration of a 3-dimensional family of boundary data $f_z(\mathbf{x})$ and $g_z(\mathbf{x})$, with \mathbf{z} being a 3D vector.

The linearized inverse problem is based on the first order approximation of (12), considering c as a small perturbation. The linearized observation equation for the first order solution \tilde{c} is deduced from (12) by leaving the right hand side of (12) unchanged and changing only the left hand side as

$$\int_{\Omega} \tilde{c} \text{grad}\phi \cdot \text{grad}\psi \, dV = \int_{\partial\Omega} (\psi f - \theta g) dS \quad (13)$$

where ϕ is the solution of the boundary value problem on the solid without defect :

$$-\text{div}\{\text{grad}\phi\} = 0 \quad (\text{in } \Omega) \quad (14)$$

$$\partial_n \phi(\mathbf{x}) = f(\mathbf{x}) \quad (\text{on } \partial\Omega) \quad (15)$$

By taking a family of boundary data $f_z(\mathbf{x})$ and $g_z(\mathbf{x})$, $\mathbf{z} \in \mathbb{R}^3$, the right hand side of (13) becomes a scalar field $d(\mathbf{z})$ and equation (13) becomes a Fredholm integral equation of the first kind for $\tilde{c}(\mathbf{x})$ with kernel $K(\mathbf{x}, \mathbf{z}) = \text{grad}_x \phi(\mathbf{x}; \mathbf{z}) \cdot \text{grad}_x \psi(\mathbf{x}; \mathbf{z})$. As expected, the linear inverse problem for \tilde{c} is ill-posed because it is governed by a Fredholm integral equation of the first kind mapping the x -space onto the z -space.

An attempt to solve the nonlinear equation has been given in (Isaacson and Isaacson, 1989) for determining $c(\mathbf{x})$ within a circular inclusion (a priori knowledge on the shape). A surprising result was found for the supporting function $\text{supp}[c]$ which takes the values 0 or 1, depending on whether $c(\mathbf{x})=0$ or $c(\mathbf{x}) \neq 0$. It is found that the support functions of $c(\mathbf{x})$ for nonlinear theory and $\tilde{c}(\mathbf{x})$ for linearized theory are practically the same. The result is very interesting for applications because it justifies the use of the linearized theory, even when $c(\mathbf{x})$ is not small.

A recent study (Bui and Constantinescu, 2000) on the detection of damage in elasticity using integral equation techniques gives a similar result. Far from the inclusion and the boundary, where $c(\mathbf{x})$ is assumed to be zero, the difference in the stress components between nonlinear and linearized theories is found to be negligible.

In the next section, we reconsider the comparison between nonlinear and linearized theories for the stationary heat equation.

3. Nonlinear and Linear Theories

Consider the inverse problem for determining an internal perturbation $c(\mathbf{x})$, using the boundary data $\theta(\mathbf{x})=h(\mathbf{x})$ and $\partial_n \theta(\mathbf{x})=f(\mathbf{x})$. Instead of comparing $c(\mathbf{x})$ with $\tilde{c}(\mathbf{x})$, we compare the nonlinear solution $\theta^{\text{NL}}(\mathbf{x})$ with the thermal field $\theta^{\text{L}}(\mathbf{x})$ associated with the linear theory. We assume

i) that the perturbation is continuous and admits a series expansion in the form $c = \varepsilon c_1 + \varepsilon^2 c_2 + \dots$ with small ε and,

ii) that the supports Z_i of the functions $c_i(\mathbf{x})$ are compact and that $c_i(\mathbf{x})=0$ on ∂Z_i and outside Z_i . The support Z of $c(\mathbf{x})$ is given by the union of the Z_i 's. A well-known example of such compact support functions is given by the test functions in finite element methods.

The field $\theta(\mathbf{x})$ satisfies the Dirichlet boundary value problem:

$$-\operatorname{div}\{(1+c)\operatorname{grad}\theta\} = 0 \quad (\text{in } \Omega) \quad (16)$$

$$\theta(\mathbf{x}) = h(\mathbf{x}) \quad (\text{on } \partial\Omega) \quad (17)$$

and admits the series expansion $\theta(\mathbf{x}) = \theta_0 + \varepsilon\theta_1(\mathbf{x}) + \varepsilon^2\theta_2(\mathbf{x}) + \dots$. The nonlinear thermal field $\theta^{\text{NL}}(\mathbf{x}) \equiv \theta(\mathbf{x})$ admits the integral representation ($\partial\theta/\partial n \equiv f(\mathbf{y})$)

$$\theta(\mathbf{x}) = \int_{\partial\Omega} \{G(\mathbf{x},\mathbf{y})f(\mathbf{y}) - h(\mathbf{y})\partial_{n_y}G(\mathbf{x},\mathbf{y})\} dS_y + \int_{\Omega} G(\mathbf{x},\mathbf{y})\operatorname{div}\{c(\mathbf{y})\operatorname{grad}\theta(\mathbf{y})\} dV_y \quad (18)$$

where $G(\mathbf{x},\mathbf{y})$ is the Green's function. We call $\theta_0(\mathbf{x})$ the zero-order solution satisfying the equations:

$$-\operatorname{div}\{\operatorname{grad}\theta_0\} = 0 \quad (\text{in } \Omega) \quad (19)$$

$$\theta_0(\mathbf{x}) = h(\mathbf{x}) \quad (\text{on } \partial\Omega) \quad (20)$$

The zero order term $\theta_0(\mathbf{x})$ admits the integral representation

$$\theta_0(\mathbf{x}) = \int_{\partial\Omega} \{G(\mathbf{x},\mathbf{y})\partial_{n_y}\theta_0(\mathbf{y}) - h(\mathbf{y})\partial_{n_y}G(\mathbf{x},\mathbf{y})\} dS_y$$

In what follows, the sum of the first two terms will be referred to as the linear solution

$$\theta^L(\mathbf{x}) = \theta_0(\mathbf{x}) + \varepsilon\theta_1(\mathbf{x}) \quad (21)$$

By substituting the series expansions of $c(\mathbf{x})$ and $\theta(\mathbf{x})$ in (16) and (17) and considering the term $O(\varepsilon)$, we obtain the governing equations for $\theta_1(\mathbf{x})$

$$-\operatorname{div}\{\operatorname{grad}\theta_1\} = \operatorname{div}\{c_1(\mathbf{x})\operatorname{grad}\theta_0(\mathbf{x})\} \quad (\text{in } \Omega) \quad (22)$$

$$\theta_1(\mathbf{x}) = 0 \quad (\text{on } \partial\Omega) \quad (23)$$

The field $\theta_1(\mathbf{x})$ admits the integral representation

$$\theta_1(\mathbf{x}) = \int_{\partial\Omega} G(\mathbf{x},\mathbf{y})\partial_{n_y}\theta_1(\mathbf{y})dS_y + \int_{\Omega} G(\mathbf{x},\mathbf{y})\operatorname{div}\{c_1(\mathbf{y})\operatorname{grad}\theta_0(\mathbf{y})\}dV_y \quad (24)$$

Using the boundary condition $c_1(\mathbf{y})=0$ on ∂Z_1 , it can be shown that the difference Δ between the nonlinear solution and the first order solution is given by

$$\begin{aligned} \Delta = \theta^{\text{NL}}(\mathbf{x}) - \theta^L(\mathbf{x}) &= \int_{\partial\Omega} G(\mathbf{x},\mathbf{y})\{\partial_{n_y}\theta - \partial_{n_y}\theta_0 - \varepsilon\partial_{n_y}\theta_1\}dS_y \\ &\quad - \varepsilon^2 \int_{Z_1} \operatorname{grad}_x G(\mathbf{x},\mathbf{y})c_1(\mathbf{y})\operatorname{grad}_y\theta_1(\mathbf{y})dV_y \end{aligned} \quad (25)$$

Both terms of the right hand side of (25) are of order $O(\varepsilon^2)$. By differentiating (25), we obtain the difference between their gradients $\Gamma = \text{grad}_x \Delta$

$$\Gamma(\mathbf{x}) = \int_{\partial\Omega} \text{grad}_x G(\mathbf{x}, \mathbf{y}) \{ \partial_{n_y} \theta - \partial_{n_y} \theta_0 - \varepsilon \partial_{n_y} \theta_1 \} dS_y - (\text{fp}) \varepsilon^2 \int_{Z_1} \text{grad}_x \text{grad}_y G(\mathbf{x}, \mathbf{y}) c_1(\mathbf{y}) \text{grad}_y \theta_1(\mathbf{y}) dV_y \quad \mathbf{x} \notin (Z_1 \cup \partial\Omega) \tag{26}$$

where (fp) stands for the Hadamard finite part sense. A close inspection of (26) shows that the difference between the thermal gradient is significant only inside or near $Z \supset Z_1$ because of the following reasons :

1. the kernel of the first term behaves as $|\text{grad}_x G| \approx |\mathbf{x} - \mathbf{y}|^{-2}$, with $|\mathbf{x} - \mathbf{y}| = \text{distance}(\mathbf{x}, \partial\Omega)$.

Therefore the first integral term is significant only in the vicinity of $\partial\Omega$, due to the difference in normal derivatives $\partial_{n_y} \theta - \partial_{n_y} (\theta_0 + \varepsilon \theta_1) \approx O(\varepsilon^2)$. Note that in the derivation of the approximate solution, $c^*(\mathbf{x})$, it is assumed that the same normal derivative holds for $\theta^L(\mathbf{x})$ and $\theta(\mathbf{x})$ so that $\{ \partial_{n_y} \theta - \partial_{n_y} (\theta_0 + \varepsilon \theta_1) \} \approx 0$.

2. the second term, understood in the Hadamard finite-part sense, decreases as $|\text{grad}_x \text{grad}_y G| \approx |\mathbf{x} - \mathbf{y}|^{-3}$, as the distance $r = \text{distance}(\mathbf{x}, Z_1)$ increases.

The difference Δ between nonlinear and linear thermal fields decreases as the distance to Z_1 increases, and the decrease of Γ is much more rapid.

These analyses show that far away from Z_1 we find that the thermal fields $\theta^{NL}(\mathbf{x})$, $\theta^L(\mathbf{x})$ and their respective gradients $\text{grad}_x \theta^{NL}(\mathbf{x})$, $\text{grad}_x \theta^L(\mathbf{x})$, are quite similar. In other words, the perturbation of the thermal coefficient $c(\mathbf{x})$ is not significant outside Z_1 , while by assumption, the perturbation $\varepsilon c_1(\mathbf{x})$ vanishes outside Z_1 , consequently vanishes too outside Z (which contains the subset Z_1).

This discussion indirectly shows that the property observed in (Isaacson and Isaacson, 1989) about the support of the nonlinear solution $c(\mathbf{x})$ for circular inclusion and that of the linearized theory $c^*(\mathbf{x})$, in the Calderon sense, Equation (13), seems to be likely for an arbitrary geometry of the inclusion.

Remark 1. The example of the thermal inverse problem shows that a relationship between the unknown coefficient $k(\mathbf{x})$ and the boundary data pair $d = \{ \theta^d, \partial_n \theta^d \}$ can be written formally as $A(k) = d$, where A is a nonlinear integral operator, the kernel of which is defined implicitly by equations (8) and (9). A simpler approximate observation equation is derived in discretized form, if we set $k = \{ k_1, k_2, k_3, \dots, k_n \}$. By means of the Finite Element Method, one solves (8) and (9) using the Neumann boundary condition $\partial_n \theta = f$ (or $\partial_n \theta^d$) and calculates the boundary temperature $\theta^{cal}(k_1, k_2, k_3, \dots, k_n)$. The inverse problem is defined as the optimization of an objective function.

Generally, the least square method is used to minimize the “error” between predicted and measured temperatures

$$k = \arg \text{Min}_k | \theta^{cal}(k_1, k_2, k_3, \dots, k_n) - \theta^d |^2$$

The difficulty of such numerical approach lies on the evaluation of the gradient of the error functional with respect to k_i which requires a great number of solutions of the equations (8) and

(9) for different increments δk_i . It can be overcome by using adjoint equations (See, e.g., Constantinescu, 1995).

Alternatively, instead of using the Neumann boundary condition, one can solve the thermal equation with the Dirichlet boundary condition $\theta=\theta^d$ and then calculate the optimal flux $\partial_n \theta^{cal}(k_1, k_2, k_3, \dots, k_n)$ which approaches the datum $\partial_n \theta^d$

$$k = \arg \text{Min}_k \left| \partial_n \theta^{cal}(k_1, k_2, k_3, \dots, k_n) - \partial_n \theta^d \right|^2$$

A symmetrical method consists of minimizing the “constitutive law error functional” (see Kohn and Vogelius, 1984 and Constantinescu, 1994, 1995).

$$F(q, \theta, k) = (1/2) \int_{\Omega} (k^{1/2} \text{grad} \theta + q k^{-1/2})^2 dV$$

where the field θ satisfies the Dirichlet boundary condition $\theta=\theta^d$ while q satisfies the equilibrium equation $\text{div}(q)=0$ and the Neumann boundary condition $q=-f$ ($k=1$ on the boundary). The constitutive law

$$q + k \text{grad} \theta = 0$$

is solution of the minimization of the “polyconvex” functional F , convex with respect to each variable separately, but not convex with respect to all together.

Remark 2. The nonlinear equation $A(u)=y, u \in X, y \in Y$ is generally solved by methods of linearization. It is assumed that the Frechet derivative $A'(u)$ exists. The least square method leads to the minimization problem $\text{Min}_u \|A(u)-y\|^2$, with the norm $\|\cdot\|$ in the Y -space. The solution is obtained formally by the multistage quadratic programming which, starting from a guess value (or a priori knowledge) u^0 , calculates the updated solution $u^{k+1}=u^k+s^k$ with

$$s^k = \text{Arg} (\text{Min}_s \|A(u^k) + A'(u^k)s - y\|^2), \quad s \in X.$$

Each stage of the calculation of s^k corresponds to a linear inverse problem $A'(u^k)s=d$, with $d=y-A(u^k)$.

4. Linear Inverse Problems Settings in Hilbert Spaces

Let X be the set of unknown model parameters and Y be the set of observable or accessible data used for recovering unknown parameters. By model parameters we include unknown mechanical fields, unknown geometry, material constants etc.

Consider two Hilbert spaces $(X, (\cdot, \cdot)_X, \|\cdot\|)$ and $(Y, (\cdot, \cdot)_Y, |\cdot|)$ with inner products $(\cdot, \cdot)_X, (\cdot, \cdot)_Y$, and respective associated norms $\|\cdot\|, |\cdot|$. We consider a continuous *linear mapping* A from X to Y , which arises in many inverse problems or in the linearisation procedure of nonlinear problems. We assume that the map A and its adjoint A^* are bounded. For given

datum $d \in Y$, one considers the problem of finding the solution of the so-called « observation equation » :

$$Au=d, \quad u \in X, \quad d \in Y \quad (27)$$

One important difference with usual direct problems is that inverse problems are generally ill-posed. This means that A is not always invertible, or solutions do not always exist, and in the case of existence of solutions, these solutions do not depend continuously on the data. The sensitivity of the solution to errors in data is the very common feature of ill-posed problems.

It is necessary to introduce a « regularization » process in order to obtain a well-posed problem, which is required to be « close » to the initial one. These two objectives – good mathematical property in the regularization process and physically acceptable model – are often so contradictory that, according to P. Sabatier (1987), their satisfaction may be rather a matter of « Art » than « Sciences ».

The equation (27) can be written in the variational form

$$(Au, Av)_Y = (d, Av)_Y, \quad u \in X, \quad d \in Y, \quad \forall v \in X \quad (28)$$

does not have an unique solution, because the bilinear form $(Au, Av)_Y$ is not assumed coercive. Regularization techniques, introduced in (Tikhonov and Arsenine, 1976, 1986), consist in the construction of « solutions » stable with respect to the variation of the datum d , by « changing » slightly the map A , or by introducing coercive variational equations.

4.1 Coercive Variational Equation

We introduce an additional term ($\alpha > 0$) in the variational equation (28)

$$(Au, Av)_Y + \alpha(u, v)_X = (d, Av)_Y, \quad u \in X, \quad \forall v \in X \quad (29)$$

The added term ensures the coercivity of the bilinear form which can be rewritten as

$$((A^*A + \alpha I)u, v)_X = (A^*d, v)_X, \quad u \in X, \quad \forall v \in X \quad (30)$$

where $(A^*A + \alpha I)$ is invertible. The solution of the modified equation (29) is

$$u(\alpha) = (A^*A + \alpha I)^{-1} A^*d \quad (31)$$

A large constant α leads to unphysical solution, while a too small value of the constant α yields unstable numerical solutions. There exists an optimal choice of the regularizing parameter, proposed by Kitagawa (1987). But this optimal choice is not essential for the following discussions. It is important to observe that if the solution u of (28) exists, the solution is unique only when A is strictly positive $A > 0$ and that the solution $u^{(\alpha)}$ in (31) with the same datum d tends towards the exact solution u in X , $\|u^{(\alpha)} - u\| \rightarrow 0$, as $\alpha \rightarrow 0$. However, in

most inverse problems for identifying defects and cracks, the condition $A > 0$ is not always satisfied.

Remark. It is worth mentioning a geometrical interpretation of the Tikhonov regularization procedure. Suppose that there is an *a priori* knowledge about the solution of (27) given by the constraint $\|u - u_0\| < \beta$ with known u_0 and $\beta > 0$. An approximate solution of (27), with an *a posteriori* residual error $\varepsilon > 0$, is given by any u belonging to the intersection C of two convexes $|Au - d| < \varepsilon$ and $\|u - u_0\| < \beta$. Either the intersection C is void (no solution to the inverse problem exists) or not void (there is an *infinite* number of approximate solutions). In the latter case, one possible solution can be chosen as follows.

Let us remark that the intersection C is bounded by two ellipsoids, $C_2 \supset C \supset C_1$, from below by the set C_1 of u such that $|Au - d|^2/\varepsilon^2 + \|u - u_0\|^2/\beta^2 \leq 1$ and from above by the set C_2 of u such that $|Au - d|^2/\varepsilon^2 + \|u - u_0\|^2/\beta^2 \leq 2$.

A solution (not unique) satisfying the constraints $|Au - d| < \varepsilon$ and $\|u - u_0\| < \beta$ is given by the common centre of C_1 and C_2 or by the solution of the minimisation problem

$$u^{(\alpha)} = \text{Arg Min}_u \{ |Au - d|^2 + \alpha \|u - u_0\|^2 \} \tag{32}$$

with $\alpha = \varepsilon^2/\beta^2$ which can be interpreted as the Lagrangian multiplier. The solution of the minimization problem (32) is unique and given by

$$u^{(\alpha)} = u_0 + (A^*A + \alpha I)^{-1} A^*(d - Au_0) \tag{33}$$

4.2 Continuity Property

Mathematically, the regularized solution $u^{(\alpha)}$ depends continuously on the datum d . This is the consequence of the Lax-Milgram theorem, based on two properties :

1. $A^*A + \alpha I$ is bounded,
2. $A^*A + \alpha I$ is coercive.

The linear operator $A^*A : X \rightarrow X$ is self-adjoint and positive, but not strictly positive. For the continuity property and the convergence property as $\alpha \rightarrow 0$, see the following Exercises.

Exercise. Prove the inequality : $\|u^{(\alpha)}(d) - u^{(\alpha)}(d')\| \leq \alpha^{-1} \|A\| \cdot |d - d'|$, for any d, d' .

Proof: Consider two data d, d' and the corresponding solutions u, u' of (29). For convenience we write simply $u = u^{(\alpha)}(d)$ and $u' = u^{(\alpha)}(d')$.

By subtracting the corresponding bilinear forms one gets:

$$\begin{aligned} (A(u - u'), Av)_Y + \alpha (u - u', v)_X &= (d - d', Av)_Y \quad \forall v \in X \\ \Rightarrow (A^*A(u - u'), v)_X + \alpha (u - u', v)_X &= (d - d', Av)_Y \quad \forall v \in X \end{aligned}$$

Take : $v = u - u'$, one gets

$$\begin{aligned} \|A^*A\| \cdot \|u - u'\|^2 + \alpha \|u - u'\|^2 &\leq \|A\| \cdot |d - d'| \cdot \|u - u'\| \Rightarrow \\ \Rightarrow \alpha \|u - u'\|^2 &\leq \|A\| |d - d'| \cdot \|u - u'\| \Rightarrow \alpha \|u - u'\| \leq \|A\| \cdot |d - d'| \quad \blacklozenge \end{aligned}$$

Exercise. (Convergence property). Prove that $\|u^{(\alpha)}(d) - u(d)\| \rightarrow 0$, as $\alpha \rightarrow 0$.

Proof: $(Au, Av)_Y = (d, Av)_Y \quad \forall v \in X$
 $(Au^{(\alpha)}, Av)_Y + \alpha(u^{(\alpha)}, v)_X = (d, Av)_Y \quad \forall v \in X$
 $(A(u^{(\alpha)} - u), Av)_Y + \alpha(u^{(\alpha)}, v)_X = 0 \quad \forall v \in X$
 Take : $v = u^{(\alpha)} - u$, one gets
 $\|A(u^{(\alpha)} - u)\|^2 + \alpha(u^{(\alpha)}, u^{(\alpha)} - u)_X = 0 \Rightarrow \alpha(u^{(\alpha)}, u^{(\alpha)} - u)_X \leq 0$
 $\Rightarrow \|u^{(\alpha)}\|^2 \leq (u^{(\alpha)}, u)_X \leq \|u^{(\alpha)}\| \cdot \|u\| \Rightarrow \|u^{(\alpha)}\| \leq \|u\|$ (34)
 Since the sequence $\|u^{(\alpha)}\|$ is bounded, there exists a subsequence converging weakly towards u , $(u^{(\alpha)} - u, v)_X \rightarrow 0, \forall v$.
 Take $v = u$ we obtain $(u^{(\alpha)} - u, u)_X \rightarrow 0$.
 Consider now:
 $\|u^{(\alpha)} - u\|^2 = (u^{(\alpha)}, u^{(\alpha)} - u)_X - (u, u^{(\alpha)} - u)_X$
 Using the inequality (34), one obtains the inequality
 $\|u^{(\alpha)} - u\|^2 \leq - (u, u^{(\alpha)} - u)_X$
 Therefore $\|u^{(\alpha)} - u\|^2 \leq - (u, u^{(\alpha)} - u)_X \rightarrow 0$ as $\alpha \rightarrow 0$, hence $\|u^{(\alpha)} - u\|^2 \rightarrow 0$.
 The sequence $u^{(\alpha)}$ converges strongly towards u ♦

4.3 Error Estimate

One important point in mathematical works is to derive the error estimate with respect to the (yet unknown) exact solution u^{ex} . There are some results reported in the literature for Inverse Problem in Hilbert spaces settings. The main point is to make a comparison between the regularized solution $u^{(\alpha)}(d)$ and the exact one u^{ex} , even if the exact solution u^{ex} is not yet known.

What is the meaning of « exact » solution ?

Let us introduce some terminologies. A pair $\{u^{\text{ex}}, d^{\text{ex}}\}$ is called *exact* or *compatible* if it satisfies the observation equation

$$Au^{\text{ex}} = d^{\text{ex}}, \quad u^{\text{ex}} \in X, \quad d^{\text{ex}} \in Y.$$

The given data d^{ex} may satisfy some *compatibility* condition for the existence of an unique *exact* solution u^{ex} in X . However it is not always possible to write explicitly the compatibility condition on d^{ex} , even if precise informations on the physical nature of the problem are known. There is of course some exception (As an example, we keep in mind the condition on the Neumann boundary data for the Laplace equation $\int_{\partial_n} u dS = 0$).

In practice, to obtain such a pair, one can take for example some u^{ex} and define d^{ex} as the direct image Au^{ex} . Such a construction of the exact pair $\{u^{\text{ex}}, d^{\text{ex}}\}$ is based on the solution of direct problems which gives indeed a compatible pair with respect to the inverse problem in consideration.

The knowledge of an exact pair, given by solutions of direct problems, is useful for checking the algorithm of approximate numerical solutions. One considers a model with known geometry and materials constants and known boundary conditions data for calculating $\{u^{\text{ex}}, d^{\text{ex}}\}$. Then one makes use of the numerical data d^{ex} for recovering the approximate numerical solution $u^{(\alpha)}$ of the inverse problem.

Another constructive solution from given data d^{ex} , consists of establishing explicit formulae giving the solution u^{ex} . Exact solutions given in Section 7 fall in this category of constructive solutions.

The main result in error estimate is stated in the following theorem.

Suppose that there exists d^1 such that $u^{\text{ex}}=A*d^1$. Then, the error $\|u^{(\alpha)}-u^{\text{ex}}\|$ is given by

$$\|u^{(\alpha)}-u^{\text{ex}}\| < (1/2) \alpha^{-1/2}(|d-d^{\text{ex}}| + \alpha|d^1|) \quad (35)$$

The proof is given in the next Exercise.

The estimate (35) depends on both the regularisation parameter α which introduces some error on the modelling and the error on the datum $|d-d^{\text{ex}}|$ in comparison with the compatible one. One gets the best possible error estimate by taking the regularization parameter proportional to the datum error $\alpha=k\varepsilon$

$$|d-d^{\text{ex}}| < \varepsilon \quad \Rightarrow \quad \|u^{(\alpha)}-u^{\text{ex}}\| < (1/2) k^{-1/2}\varepsilon^{1/2}(1+k|d^1|)$$

Exercise. Suppose that there exists d^1 such that $u^{\text{ex}}=A*d^1$, prove the estimate (35).

Proof: The exact pair $(u^{\text{ex}}, d^{\text{ex}})$ satisfies the variational equation

$$(Au^{\text{ex}}, Av)_Y = (d^{\text{ex}}, Av)_Y \quad \forall v \in X, \quad (36)$$

The approximate solution $(u^{(\alpha)}, d)$ satisfies the equation

$$(Au^{(\alpha)}, Av)_Y + \alpha(u^{(\alpha)}, v)_X = (d, Av)_Y \quad \forall v \in X$$

which can be written as :

$$(Au^{(\alpha)}, Av)_Y + \alpha(u^{(\alpha)}-u^{\text{ex}}, v)_X + \alpha(u^{\text{ex}}, v)_X = (d, Av)_Y \quad \forall v \in X \quad (37)$$

Combining (36) and (37) we get :

$$(A(u^{(\alpha)}-u^{\text{ex}}), Av)_Y + \alpha(u^{(\alpha)}-u^{\text{ex}}, v)_X + \alpha(u^{\text{ex}}, v)_X = (d-d^{\text{ex}}, Av)_Y \quad \forall v \in X$$

Take $v= u^{(\alpha)}-u^{\text{ex}}$, one obtains

$$\begin{aligned} |A(u^{(\alpha)}-u^{\text{ex}})|^2 + \alpha\|u^{(\alpha)}-u^{\text{ex}}\|^2 &= (d-d^{\text{ex}}, A(u^{(\alpha)}-u^{\text{ex}}))_Y \\ &- \alpha(u^{\text{ex}}, u^{(\alpha)}-u^{\text{ex}})_X \end{aligned} \quad (38)$$

The last term can be written as

$$\alpha(u^{\text{ex}}, u^{(\alpha)}-u^{\text{ex}})_X = \alpha(A*d^1, u^{(\alpha)}-u^{\text{ex}})_X = \alpha(d^1, A(u^{(\alpha)}-u^{\text{ex}}))_Y$$

The left hand side of (38) is bounded by

$$\begin{aligned} |A(u^{(\alpha)}-u^{\text{ex}})|^2 + \alpha\|u^{(\alpha)}-u^{\text{ex}}\|^2 &\leq |d-d^{\text{ex}}| \cdot |A(u^{(\alpha)}-u^{\text{ex}})| \\ &+ \alpha|d^1| \cdot |A(u^{(\alpha)}-u^{\text{ex}})| \leq |A(u^{(\alpha)}-u^{\text{ex}})| \cdot (|d-d^{\text{ex}}| + \alpha|d^1|) \\ &\leq |A(u^{(\alpha)}-u^{\text{ex}})|^2 + (1/4) (|d-d^{\text{ex}}| + \alpha|d^1|)^2 \end{aligned}$$

Finally, by using $|d-d^{\text{ex}}| < \varepsilon$ and $\alpha=k\varepsilon$, one obtains the inequality (35)

$$\begin{aligned} \alpha\|u^{(\alpha)}-u^{\text{ex}}\|^2 &\leq (1/4) (|d-d^{\text{ex}}| + \alpha|d^1|)^2 \\ \Rightarrow \|u^{(\alpha)}-u^{\text{ex}}\| &\leq (1/2) \alpha^{-1/2} (|d-d^{\text{ex}}| + \alpha|d^1|) \quad \blacklozenge \end{aligned}$$

5. Geometry Bound Methods for Static Problems

It is often of interest to determine, not exactly the geometry of defects and cracks, but only their approximate location in the solid. Geometry bound methods consist of determining spatial subdomains which do not contain internal defects and cracks. The initial inverse problem of determining defects or cracks in Ω , using the boundary data pairs $\{u, \partial_n u\}$ for Laplace's